# Nonlinear slope-dependent sediment transport in cinder cone evolution

Jon D. Pelletier*
Michael L. Cline
Department of Geosciences, University of Arizona, Gould-Simpson Building, 1040 East Fourth Street, Tucson, Arizona 85721–0077, USA

## ABSTRACT

**Sediment flux on transport-limited hillslopes is well known to vary nonlinearly with slope, diverging as the angle of stability is approached. To date, however, no study has validated the precise form of the nonlinear slope-dependent transport model over geologic time scales in a non-steady-state landform. In this paper, we show how cinder cones can be used to validate the nonlinear transport model using Lathrop Wells cinder cone in Nye County, Nevada, as a type example. Cinder cones are well suited for this purpose because they can be radiometrically dated and their angles of stability can be constrained by measurement of subsurface contacts between primary fallout and overlying colluvial deposits reworked from upslope. Forward model results with a generalized, nonlinear transport model characterized by diffusivity, κ, and nonlinear exponent, *n*, show that the evolution of the cone rim and base are most sensitive to κ, while the cone midpoint is most sensitive to *n*. Analyses of the full cone shape, therefore, permit the two model parameters to be independently inferred if the cone age and angle of stability are independently known. Results for Lathrop Wells imply that *n* = 2 in the generalized, nonlinear transport model, which is consistent with Roering et al.'s (1999) widely used form of that model.**

**Keywords:** hillslope evolution, nonlinear diffusion, cinder cones, numerical model.

## INTRODUCTION

The evolution of transport-limited hillslopes is a classic problem in geomorphology. Culling (1960, 1963) first proposed the use of the diffusion equation to model the evolution of gently sloping hillslopes subject to stepwise transport processes such as creep, rainsplash, and bioturbation. The diffusion model in its simplest form is limited in two primary ways, however. First, it fails to account for regolith-depth-dependent transport processes (Gabet, 2000; Heimsath et al., 2005); hence it is best applied to landforms with a thick cover of unconsolidated material. Second, the diffusion model fails to account for the increase in sediment flux as hillslopes steepen and mass movements become the dominant mode of transport. Mass movements can be quantified with a nonlinear increase in sediment flux as the angle of stability is approached. Most nonlinear hillslope-evolution models that aim to model both gentle-sloping and steep terrain, therefore, follow the general form

$$\frac{\partial h}{\partial t} = \nabla \cdot q_s = \kappa \nabla \cdot \left( \frac{\nabla h}{1 - \left( |\nabla h| / S_c \right)^n} \right), \quad (1)$$

where $h$ is elevation, $t$ is time following the initial condition, $q_s$ is sediment flux, κ is the diffusivity constant, and $S_c$ is the tangent of the angle of stability. Equation 1 reduces to the diffusion equation for $|\nabla h| << S_c$. For $|\nabla h| \approx S_c$, Equation 1 predicts nonlinearly increasing sediment flux as $S_c$ is approached. The exponent $n$ quantifies how quickly the transition between linear and nonlinear slope-dependent processes occurs (Fig. 1A). In the context of pluvial shoreline and fault-scarp evolution, Andrews and Hanks (1985) used Equation 1 with $n = 1$, while Andrews and Bucknam (1987) and Mattson and Bruhn (2001) adopted $n = 2$. Small-scale experiments, post-disturbance sediment-yield data, and analyses of steady-state hillslope morphology all support the value $n = 2$ (Roering et al., 1999; 2001a, 2001b; Gabet, 2003; Roering and Gerber, 2005). Recent theoretical modeling, however, suggests that $n$ may be a function of the depth profile of sediment in motion (Roering, 2004) and hence may not be universal. High-magnitude earthquakes could initiate flow deeper in the regolith profile, for example, resulting in lower values of $n$. Also, no study has conclusively verified Equation 1 for any particular value of $n$ for a non-steady-state landform. The distinction between steady-state and non-steady-state landforms is significant because topographic steady state is difficult to verify at the hillslope scale and because certain non-steady-state conditions can predict the same hillslope morphologies in the linear diffusion model as occur in the nonlinear model under the assumption of steady state (Jimenez-Hornero et al., 2005). Studies of fault and pluvial shoreline scarps have successfully used Equation 1 for many years, but linearly slope-dependent transport models have also been successful in characterizing scarp evolution (e.g., Pelletier et al., 2006), largely because the local angle of stability in fault and shoreline scarps is not precisely known.

In this paper, we show how analyses of cinder cone morphology provide a unique opportunity to calibrate all of the parameters of the nonlinear slope-dependent transport model for a non-steady-state landform. Cinder cones are ideal natural laboratories for studying hillslope evolution in steep terrain because they can be radiometrically dated, their angles of stability can be inferred directly from subsurface contacts, and because they form at or near the angle of stability. In addition, cinder cones are comprised of well-sorted, cohesionless parent material, thus minimizing the influence of textural variability on model inference.

## NUMERICAL MODEL

For radially symmetric landforms, Equation 1 becomes

$$\frac{\partial h}{\partial t} = \frac{\kappa}{r} \frac{\partial}{\partial r} \left( \frac{r \frac{\partial h}{\partial r}}{1 - \left( \frac{\left| \partial h / \partial r \right|}{S_c} \right)^n} \right), \quad (2)$$

where $r$ is the distance from the center of the landform. Equation 2 can be readily solved numerically using upwind differencing in space and a predictor-corrector method in time (Press et al., 1992). Hooper and Sheridan (1998) first modeled cone evolution using linear and nonlinear slope-dependent transport models. These authors compared the modeled midpoint slope to measured values on cones of different ages, but they did not interpret or analyze the entire cone shape.

Figure 1B illustrates the evolution of a cinder cone evolving according to Equation 1 with an initial slope of 32.99°, $n = \infty$, and $S_c = 33°$ at $\kappa t = 100, 200, 400, \ldots 3200$ m$^2$. The initial shape is further defined by an initial cone radius $r_c$, rim radius $r_r$, and colluvial fill radius $r_f$ (equal to 350, 100, and 50 m, respectively, in Figures 1B and 1C). In the limit $n = \infty$, Equation 2 reduces to the linear diffusion equation because the initial slope angle is below the angle of stability everywhere along the profile, and nonlinearity only occurs when the slope angle equals

*E-mail: jdpellet@email.arizona.edu.

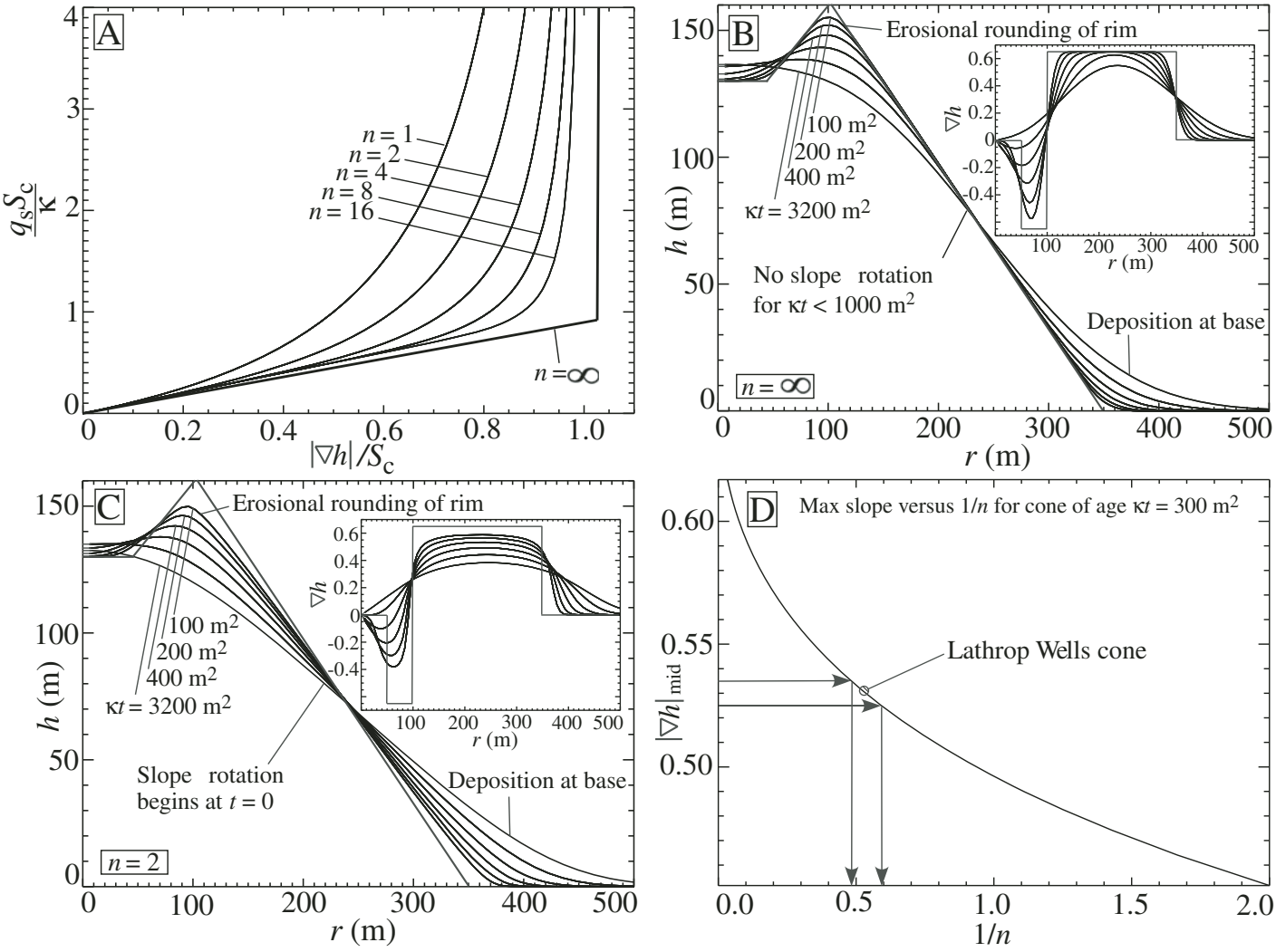


**Figure 1. A: Plot of normalized sediment flux versus normalized slope for the nonlinear slope-dependent transport model (Equation 1). The value of the exponent *n* in this model characterizes how rapidly nonlinear transport increases sediment flux as the angle of stability, $S_c$, is approached. B: Plots of radial-profile evolution of a cinder cone evolving according to Equation 1 with $n = \infty$ and an initial morphology similar to Lathrop Wells cone. The evolution is characterized by rounding of the cone rim and base (where curvature is concentrated) and stability of the midpoint for times less than $\kappa t \approx 1000$ m². C: Same as B but with $n = 2$. In this case, rounding of rim and base is accompanied by a slope "rotation" component driven by nonlinear transport close to the angle of stability. D: Relationship between midpoint slope and 1/*n* for a cone with an initial geometry similar to Lathrop Wells cone, an initial angle of 33°, and an age of $\kappa t = 300$ m².**

$\tan^{-1}(S_c)$ in that limit. In this case, erosion and deposition are concentrated at the cone rim and base where the curvatures are greatest. For cones younger than $\kappa t \approx 1000$ m², the midpoint slope angle is unchanged from its initial value. As a validation of the numerical model, the results in Figure 1B were compared with those of semi-analytical solutions to the linear diffusion equation obtained with a Fourier-Bessel series expansion (Appendix DR1 in the GSA Data Repository[1]).

Figure 1C illustrates the modeled cone evolution for the same initial condition as Figure 1B, but with $n = 2$ (first proposed by Andrews and Bucknam [1987], recently studied in detail by Roering et al. [1999; 2001a; 2001b]). In this case, the rim and base erode and deposit in a manner very similar to that of Figure 1B, but this model also includes a slope "rotation" component that causes the midpoint slope angle to decrease significantly, beginning immediately following the eruption. This slope rotation reflects the rapid sediment transport caused by mass movements at angles close to the angle of stability. These results suggest that the relationship between sediment flux and slope can be inferred from an analysis of the full cone shape, if the age of the cone and the angle of stability are known (thereby reducing a four-parameter model to a two-parameter model). Figure 1 shows that the value of $\kappa$ is most sensitive to the degree of rounding at the rim and base of the cone, while the value of *n* is most sensitive to the extent of slope rotation at the cone midpoint.

## APPLICATION TO LATHROP WELLS, NYE COUNTY, NEVADA

Lathrop Wells cone has been the subject of intense study as a natural analog site for a potential volcanic eruption through the proposed nuclear waste repository at Yucca Mountain. The cone, radiometrically dated to be 77 ka (Heizler et al., 1999), is located near the southern boundary of the Nevada Test Site in Nye County, Nevada. Field observations indicate that most of the cone was deposited during one major, violent, Strombolian eruption phase (Valentine et al., 2005). The cone is predominantly

[1]GSA Data Repository item 2007266, semi-analytic solutions to the diffusion equation for cinder cone evolution, is available online at www.geosociety.org/pubs/ft2007.htm, or on request from editing@geosociety.org or Documents Secretary, GSA, P.O. Box 9140, Boulder, CO 80301, USA.

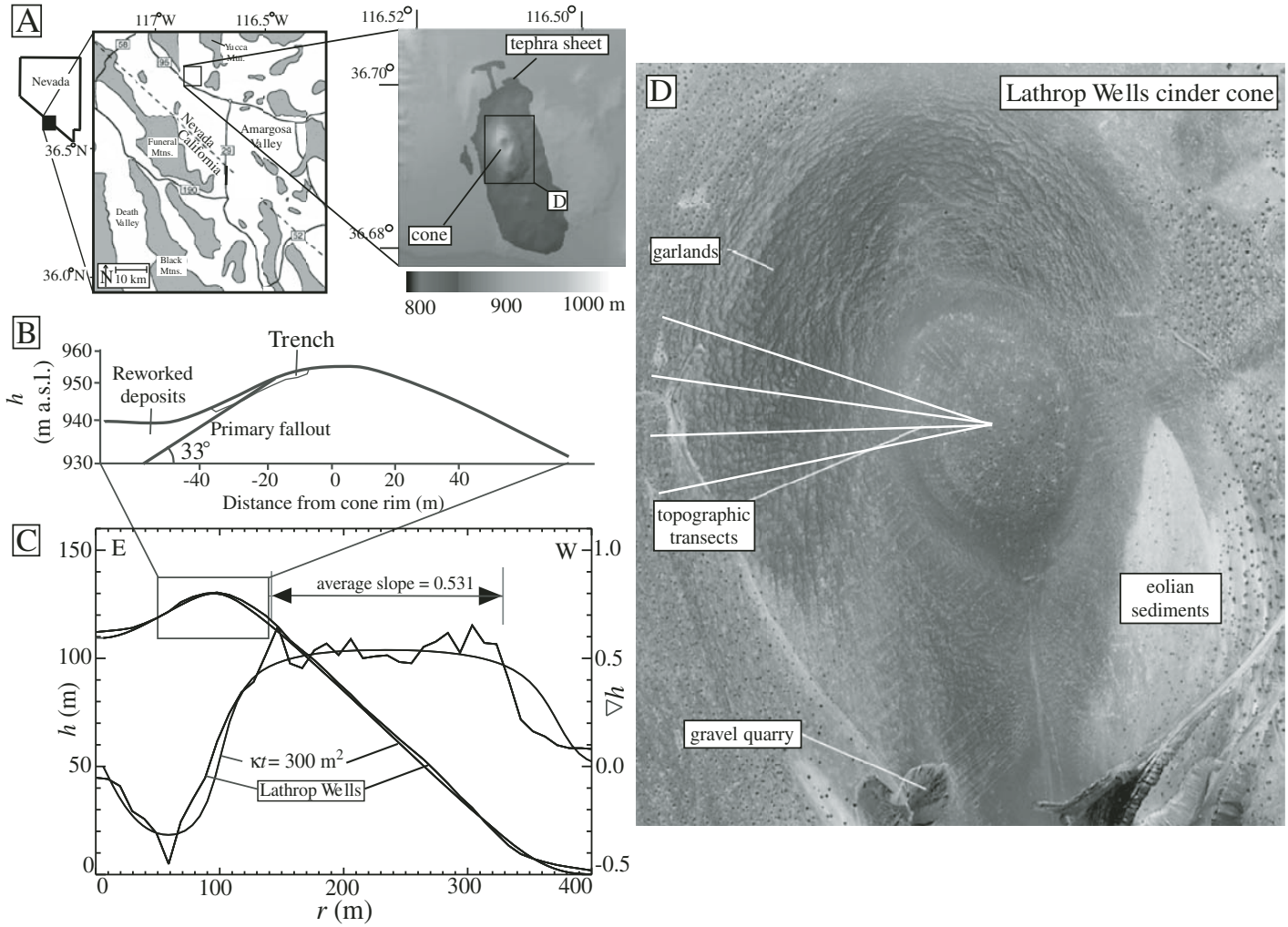


**Figure 2. A: Location map of Lathrop Wells cone, Nye County, Nevada. Also shown is image of digital elevation model (DEM) with cone and tephra-sheet extent identified in transparent overlay. B: Schematic cross section of cone rim along an east-to-west profile, showing location of trench and 33° contact between primary cone and reworked deposits (after SNL, 2007). C: Topographic (elevation and slope) transects of Lathrop Wells cone from east to west originating at the cone center. The best-fit match between the model and observed profiles occurs for $\kappa t$ = 300 m² and $n$ = 2. D: Aerial photograph of Lathrop Wells cone prior to extensive quarrying, showing principal surface features and locations of topographic transects used in the analysis (after SNL, 2007).**

composed of loose, well-sorted, vesicular scoria lapilli with a median grain diameter of 8 mm (SNL, 2007). Eolian sand deposits occur locally near the base of the cone, but overall, the coarse texture and general absence of significant eolian dust deposition minimize runoff generation, water storage in the subsurface, and vegetation cover on the cone. As such, the dominant transport mechanism is most likely seismically induced dry ravel. This hypothesis is supported by observations of lenticularly shaped, inversely graded, avalanche deposits exposed near the base of the cone (SNL, 2007). Seismicity in the Yucca Mountain region has been well documented (CRWMS M&O, 1998), including displaced or disturbed alluvial and colluvial deposits of late Quaternary age on nine faults and the 1992 M5.6 Little Skull Mountain earthquake that occurred 11 km from Lathrop Wells. The only significant microtopographic features on Lathrop Wells are the large-scale "ripples" oriented parallel to contour lines, called garlands, which have heights of several decimeters, wavelengths of five to ten meters, and crestlines composed of preferentially coarse tephra (Fig. 2D). The origin of these features is not precisely known, but laboratory studies of granular materials subject to horizontal vibration commonly form texturally segregated, ripple-like bedforms similar to garlands (Ciamarra et al., 2005).

Perry et al. (1998) dug an east-west–oriented trench near the cone rim and observed the contact between primary fallout deposits and reworked colluvial deposits to be 33°. This contact preserves the initial angle of the slope immediately following eruption and provides an important data point for our analysis because it directly constrains the angle of stability of the cone, $\tan^{-1}(S_c)$. By comparing the present-day midpoint slope to the initial angle of 33°, we can infer the extent of the slope "rotation" component of cone evolution, illustrated in Figure 1C, which, in turn, is diagnostic of the nonlinear portion of the sediment-flux relationship plotted in Figure 1A. It should be noted that trenches of fault and pluvial shoreline scarps may also preserve the initial scarp shape, but in those cases, the initial angle represents the angle of faulting or the angle of stability under continuous wave-cut action, neither of which may be equal to the angle of stability following scarp formation. The 33° angle measured by Perry et al. (1998) is coincident with the commonly assumed value for $\tan^{-1}(S_c)$ in fault scarp and pluvial shoreline studies (e.g., Andrews and Hanks, 1985). Experiments show, however, that angles of stability in cohesionless material vary between 28° and 42°, depending on grain size and shape (Simons and Albertson, 1963); therefore, a direct measurement of the local value of $S_c$ is necessary to be certain of the extent of slope rotation.

Figure 2C illustrates the best-fit relationship between the nonlinear slope-dependent transport model and the observed western topographic profile of Lathrop Wells. The overall cone shape is slightly asymmetric in map view (likely due to southerly winds during eruption); therefore, it is most appropriate to compare the angle of stability measured by Perry et al. (1998) to the present-day slope angle along the same east-west–oriented profile where the subsurface contact was measured in the trench. The best-fit model result corresponds to $\kappa t = 300$ m$^2$ (i.e., $\kappa = 3.9$ m$^2$/kyr, which is consistent with the upper range of values inferred from pluvial shoreline and fault scarps in the southwestern United States (Hanks, 2000)) and $n = 2$. The best-fit model was deduced by first varying the value of $\kappa$ to fit the degree of rounding of the cone rim (which depends only weakly on $n$), and then varying $n$ to fit the extent of slope rotation. The best-fit value of $n$ can be pinpointed most precisely using the sensitivity plot shown in Figure 1D. This plot represents the midpoint slope of a cone starting from 33° with age $\kappa t = 300$ m$^2$ as a function of $1/n$. This plot was constructed by forward modeling many hypothetical Lathrop Wells cones, each with a different value of $n$, to an age of $\kappa t = 300$ m$^2$. Figure 1D shows that as $n \rightarrow \infty$ (or $1/n$ goes to zero), the midpoint slope approaches the initial value of tan(33°) or 0.65. This result is consistent with the evolution shown in Figure 1B, in which the midpoint slope is insensitive to age for a young cone in the large $n$ limit. As the value of $n$ decreases (or $1/n$ increases), the midpoint slope of the cone decreases from tan(33°) (0.65) at $n = \infty$, to tan(28°) (0.53) at $n = 2$, to tan(26.5°) (0.50) at $n = 1$. Four topographic profiles measured along the western slope were extracted from the U.S. Geological Survey 10-m-resolution Digital Elevation Model (Fig. 2D). Each profile was differentiated to obtain a corresponding slope profile (e.g., Fig. 2C). An average slope for the straight midpoint segment of each profile was calculated for each profile to yield an average value of $0.531 \pm 0.004$ for the four profiles. This range of slope values corresponds to $n = 1.9 \pm 0.2$ (Fig. 1D), which is consistent with Roering's widely used form of the generalized nonlinear slope-dependent transport model.

## CONCLUSIONS

Cinder cones provide an unusual opportunity to precisely constrain the initial condition of a landform at a known time in the geologic past. Using published radiometric ages and measurement of subsurface contacts, forward modeling of cone evolution and comparison with present-day profiles can constrain the precise form of the nonlinear relationship between sediment flux and slope. The results for Lathrop Wells cinder cone confirm the nonlinear transport model with $n = 2$. It should be noted, however, that young cinder cones are, by nature, predominantly comprised of cohesionless material subject to dry ravel. Therefore, more work is needed to test the nonlinear transport model with $n = 2$ in non-steady-state landforms with a range of substrate textures and cohesive strengths where processes other than dry ravel are dominant.


## ACKNOWLEDGMENTS

We thank Greg Valentine for helpful discussions during a field trip to Lathrop Wells. We also thank Josh Roering and two anonymous reviewers for helpful comments.


## REFERENCES CITED


Andrews, D.J., and Bucknam, R.C., 1987, Fitting degradation of shoreline scarps by a nonlinear diffusion model: Journal of Geophysical Research, v. 92, p. 12,857–12,867.

Andrews, D.J., and Hanks, T.C., 1985, Scarp degraded by linear diffusion: Inverse solution for age: Journal of Geophysical Research, v. 90, p. 10,193–10,208.

Ciamarra, M.-P., Coniglio, A., and Nicodemi, M., 2005, Shear instabilities in granular mixtures: Physical Review Letters, v. 94, art. 188001.

CRWMS M&O (Civilian Radioactive Waste Management System Management and Operating Contractor), 1998, Yucca Mountain Site Description: Report No. B00000000–01717–5700–00019, Rev 0: CRWMS M&O, Las Vegas, Nevada.

Culling, W.E.H., 1960, Analytical theory of erosion: The Journal of Geology, v. 68, p. 336–344.

Culling, W.E.H., 1963, Soil creep and the development of hillside slopes: The Journal of Geology, v. 71, p. 127–161.

Gabet, E.J., 2000, Gopher bioturbation: Field evidence for nonlinear hillslope diffusion: Earth Surface Processes and Landforms, v. 25, p. 1419–1428, doi: 10.1002/1096–9837(200012)25:13<1419:AID-ESP148>3.0.CO;2–1.

Gabet, E.J., 2003, Sediment transport by dry ravel: Journal of Geophysical Research, v. 108, no. B1, doi: 10.1029/2001JB001686.

Hanks, T.C., 2000, The age of scarplike landforms from diffusion equation analysis, *in* Noller, J.S., Sowers, J.M., and Lettis, W.R., eds., Quaternary geochronology, methods and applications: American Geophysical Union, Washington, D.C., p. 313–338.

Heimsath, A.M., Furbish, D.J., and Dietrich, W.E., 2005, The illusion of diffusion: Field evidence for depth-dependent sediment transport: Geology, v. 33, p. 949–952, doi: 10.1130/G21868.1.

Heizler, M.T., Perry, F.V., Crowe, B.M., Peters, L., and Appelt, R., 1999, The age of the Lathrop Wells volcanic center: An $^{40}Ar/^{39}Ar$ dating investigation: Journal of Geophysical Research, v. 104, p. 767–804, doi: 10.1029/1998JB900002.

Hooper, D.M., and Sheridan, M.F., 1998, Computer simulation models of scoria cone degradation: Journal of Volcanology and Geothermal Research, v. 83, p. 241–267, doi: 10.1016/S0377–0273(98)00031–6.

Jimenez-Hornero, F.J., Laguna, A., and Giraldez, J.V., 2005, Evaluation of linear and nonlinear sediment transport equations using hillslope morphology: CATENA, v. 64, p. 272–280, doi: 10.1016/j.catena.2005.09.001.

Mattson, A., and Bruhn, R.L., 2001, Fault slip rates and initiation age based on diffusion equation modeling: Wasatch fault zone and eastern Great Basin: Journal of Geophysical Research, v. 106, p. 13,739–13,750, doi: 10.1029/2001JB900003.

Pelletier, J.D., DeLong, S., Al Suwaidi, A.H., Cline, M.L., Lewis, Y., Psillas, J.L., and Yanites, B., 2006, Evolution of the Bonneville shoreline scarp in west-central Utah: Comparison of scarp-analysis methods and implications for the diffusion model of hillslope evolution: Geomorphology, v. 74, p. 257–270, doi: 10.1016/j.geomorph.2005.08.008.

Perry, F.V., Crowe, B.M., Valentine, G.A., and Bowker, L.M., 1998, Volcanism studies: Final report for the Yucca Mountain Project: LANL Report LA-13478: Los Alamos National Laboratory, Los Alamos, New Mexico, 554 p.

Press, W.H., Flannery, B.P., Teukolsky, S.A., and Vetterling, W.T., 1992, Numerical recipes in C, 2nd edition: New York, Cambridge University Press, 994 p.

Roering, J.J., 2004, Soil creep and convex-upward velocity profiles: Theoretical and experimental investigation of disturbance-driven sediment transport on hillslopes: Earth Surface Processes and Landforms, v. 29, p. 1597–1612, doi: 10.1002/esp.1112.

Roering, J.J., and Gerber, M., 2005, Fire and the evolution of steep, soil-mantled landscapes: Geology, v. 33, p. 349–352, doi: 10.1130/G21260.1.

Roering, J.J., Kirchner, J.W., and Dietrich, W.E., 1999, Evidence for nonlinear, diffusive sediment transport on hillslopes and implications for landscape morphology: Water Resources Research, v. 35, p. 853–870, doi: 10.1029/1998WR900090.

Roering, J.J., Kirchner, J.W., and Dietrich, W.E., 2001a, Hillslope evolution by nonlinear, slope-dependent transport: Steady-state morphology and equilibrium adjustment timescales: Journal of Geophysical Research, v. 106, p. 16,499–16,513, doi: 10.1029/2001JB000323.

Roering, J.J., Kirchner, J.W., Sklar, L.S., and Dietrich, W.E., 2001b, Hillslope evolution by nonlinear creep and landsliding: An experimental study: Geology, v. 29, p. 143–146, doi: 10.1130/0091–7613(2001)029<0143:HEBNCA>2.0.CO;2.

Simons, D.B., and Albertson, M.E., 1963, Uniform water conveyance channels in alluvial material: Transactions of the American Society of Civil Engineers, v. 128, p. 65–108.

SNL (Sandia National Laboratory), 2007, Characterize eruptive processes at Yucca Mountain: Report ANL-MGR-GS-000002 Rev 003, Sandia National Laboratory, Las Vegas, Nevada, 252 p.

Valentine, G.A., Krier, D.J., Perry, F.V., and Heiken, G., 2005, Scoria cone construction mechanisms, Lathrop Wells scoria cone volcano, southern Nevada, USA: Geology, v. 33, no. 8, p. 629–632.



Manuscript received 23 April 2007
Revised manuscript received 2 July 2007
Manuscript accepted 15 July 2007

Printed in USA